An Experimental Study of the Thermodynamic Properties of Multicomponent Polyolefin Blends with Ordered and Disordered Phases

H. S. Jeon, J. H. Lee, N. P. Balsara,* and M. C. Newstein

Departments of Chemical Engineering, Chemistry, Materials Science, and Electrical Engineering, Polytechnic University, Six Metrotech Center, Brooklyn, New York 11201

Received July 1, 1997; Revised Manuscript Received March 4, 1998

ABSTRACT: Concentration fluctuations and phase transitions in multicomponent polymer blends comprising polyethylene (PE), head-to-head polypropylene (PP), and a symmetric PE−PP diblock copolymer were studied by a combination of light and neutron scattering. When the block copolymer concentration was below a certain threshold (12.5 vol % in our system), the blends exhibited macrophase separation. At higher block copolymer concentrations, we found stable, periodic structures that were characterized by a neutron scattering peak at finite scattering vector, q. In this regime, the block copolymer serves as a surfactant. At high block copolymer concentrations, ordered microphases that were similar to those found in pure block copolymer melts were obtained. At lower block copolymer concentrations, however, microemulsions that are periodic phases that lack long-range order were obtained. Concentration fluctuations of individual components in these multicomponent mixtures in the single-phase regime were examined by conducting neutron scattering experiments on contrast-matched systems. The formation of disordered phases and microemulsions is announced by transient, intermolecular aggregation of the homopolymers. In contrast, the formation of ordered structures is announced by both intermolecular and intramolecular signatures. Many of our results are in quantitative agreement with theoretical predictions based on the random phase approximation.

Introduction

In the preceding paper,[1] which we refer to as paper I, we began a systematic study of concentration fluctuations and phase transitions in multicomponent mixtures of model polyolefins: polyethylene (PE), head-to-head polypropylene (PP) and a symmetric PE−PP diblock copolymer. Neutron-scattering experiments were conducted on a critical, binary PE/PP blend ($\phi_{PE}/\phi_{PP} = 1.63$, ϕ_i is the volume fraction of component i in the blend) and the pure PE−PP block copolymer. The Flory−Huggins interaction parameter between PE and PP chains, and the statistical segment lengths of the homopolymer and copolymer chains were estimated by fitting the measured neutron-scattering profiles from these systems to theoretical predictions based on the random phase approximation (RPA). The RPA is only applicable in the single-phase regime. We then used the multicomponent RPA to compute the scattering profiles from PE/PP/PE−PP blends with $\phi_{PE}/\phi_{PP} \approx 1.6$ and ϕ_{PE-PP} ranging from 0.05 to 0.75. When the block copolymer concentration was low ($\phi_{PE-PP} \leq 0.05$), we found monotonic scattering profiles, with scattering maxima in the forward direction. This behavior is typical of simple, binary liquids, and we therefore expected multicomponent blends with $\phi_{PE-PP} \leq 0.05$ to exhibit macrophase separation. When the block copolymer concentration was high ($\phi_{PE-PP} \geq 0.30$), we found scattering profiles with well-defined peaks at finite scattering angles and negligible scattering in the forward direction. This behavior is typical of pure block copolymers, and we therefore expected multicomponent blends with $\phi_{PE-PP} \geq 0.30$ to exhibit microphase separation. At intermediate block copolymer concentrations ($\phi_{PE-PP} = 0.10$) we observed complex behavior. The scattering profiles from these blends contained peaks at finite scattering angle, but the scattering intensity in the forward direction was nonnegligible. As the phase transition temperature was approached, the scattering intensity at the peak as well as that in the forward direction increased rapidly. Multicomponent blends in the vicinity of $\phi_{PE-PP} = 0.10$ are thus seen to exhibit characteristics of both macrophase as well as microphase separation.

The objective of this paper, which we refer to as paper II, is to present experimental data from multicomponent PE/PP/PE−PP blends and compare them with the theoretical predictions described above. Concentration fluctuations of individual components in single-phase blends were studied by conducting neutron-scattering experiments on contrast-matched systems. The microstructure of phase-separated blends was studied by a combination of neutron scattering and light-scattering. As anticipated by theory, we find that these blends exhibit macrophase separation at low block copolymer concentrations. On the other hand, phase separation in blends with high block copolymer concentrations leads to the formation of ordered microphases. At intermediate block copolymer concentrations, however, phase separation leads to the formation of microemulsions which are periodic structures that lack long-range order.

Experimental Section

Polyethylene (PE) and head-to-head polypropylene (PP) homopolymers and PE−PP diblock copolymers were synthesized by methods described in paper I.[1] The chemical structures of PE and PP monomers are given in Figure 1. Two sets of polyolefins were synthesized: a set of fully hydrogenous polyolefins (hPE, hPP, and hPE−hPP) and a set of partially deuterated polyolefins (dPE, dPP, and dPE−dPP). The characteristics of these polymers are summarized in Table 1. Blends of two homopolymers and a block copolymer were made by the procedure described in paper I. In this paper, we discuss the properties of two series of multicomponent blends labeled BH and BB. Blends labeled BH are composed of hPE, dPP, and hPE−hPP, while blends labeled BB are composed

S0024-9297(97)00972-8 CCC: $15.00
Published on Web 04/29/1998

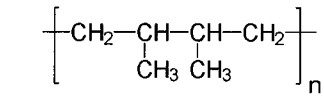

Head-to-Head Polypropylene (PP)

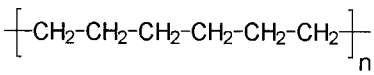

Polyethylene (PE)

Figure 1. Chemical structure of monomers of head-to-head polypropylene (PP) and polyethylene (PE) chains.

Table 1. Characteristics of Polyolefins

sample designation	mol wt (wt av)[a] (kg/mol)	polydispersity index[b]	vol fr of PE in block copolymer[c]	density[d] (gm/cm^3)	av no. of deuterium per C_6 monomer[e]
hPE	7.0	1.04		0.9275	0
dPE	7.4	1.04		0.9865	5.24
hPP	15	1.10		0.8744	0
dPP	16	1.09		0.9321	5.43
hPE−hPP	63	1.12	0.49	0.8973	0
dPE−dPP	66	1.12	0.49	0.9476	4.51

[a] From light scattering from dilute solutions of polydienes. [b] From high-temperature GPC. [c] Based on ^{13}C NMR. [d] From density measurements using a density gradient column. [e] Based on density measurements.

Table 2. Composition of the Multicomponent Blends Examined

blend designation	components			compositions	
	A	B	A−B	ϕ_A/ϕ_B (ϕ_A)	ϕ_{A-B}
BH05	hPE	dPP	hPE−hPP	1.6298 (0.5890)	0.0496
BH10	hPE	dPP	hPE−hPP	1.6379 (0.5588)	0.1001
BH15	hPE	dPP	hPE−hPP	1.6306 (0.5275)	0.1489
BH20	hPE	dPP	hPE−hPP	1.6191 (0.4948)	0.1996
BH30	hPE	dPP	hPE−hPP	1.6256 (0.4334)	0.3000
BH50	hPE	dPP	hPE−hPP	1.6188 (0.3055)	0.4946
BH75	hPE	dPP	hPE−hPP	1.6188 (0.1554)	0.7486
BB05	hPE	hPP	dPE−dPP	1.6279 (0.5880)	0.0507
BB10	hPE	hPP	dPE−dPP	1.5482 (0.5465)	0.0982
BB20	hPE	hPP	dPE−dPP	1.6331 (0.4958)	0.2006
BB30	hPE	hPP	dPE−dPP	1.6247 (0.4338)	0.2992
BB50	hPE	hPP	dPE−dPP	1.5466 (0.3056)	0.4968
BB75	hPE	hPP	dPE−dPP	1.6087 (0.1546)	0.7493

of hPE, hPP, and dPE−dPP. The volume fraction ratio, ϕ_{PE}/ϕ_{PP}, was fixed at about 1.6 in both BH and BB series. Individual blends are labeled either BH*ij* or BB*ij* where *ij* is the nominal volume percent of block copolymer in the blend. Blends were made in pairs (except for BH15), each BH*ij* has a corresponding BB*ij*. Each pair consists of blends that are identical in composition, except for the fact that the labeled species in the BH*ij* blend is the PP homopolymer, while the labeled species in the BB*ij* blend is the block copolymer. Since the neutron-scattering contrast between the hydrogenous polyolefins is negligible, blend BH*ij* enables the study of concentration fluctuations of the PP homopolymer, while blend BB*ij* enables the study of concentration fluctuations of the block copolymer. The exact composition of the blends used in this study are given in Table 2.

Small angle neutron-scattering (SANS) experiments were conducted on the 8 m SANS machine on the NG5 beam line, and the 30 m SANS machine on the NG3 beam line at National Institute of Standards and Technology in Gaithersburg, MD. The blends were encased in quartz cells with a 1 mm path length. The configuration of the 8 m SANS machine was neutron wavelength $\lambda = 12.0$ Å, wavelength spread $\Delta\lambda/\lambda = 0.25$, sample-to-detector distance = 3.6 m, sample aperture = 1.2 cm, source-to-sample distance = 4.1 m, and source size = 2.7 cm. The configuration of the 30 m SANS machine was neutron wavelength $\lambda = 14.0$ Å, wavelength spread $\Delta\lambda/\lambda = 0.15$, sample-to-detector distance = 13.17 m, sample aperture = 1.2 cm, source-to-sample distance = 11 m, and source diameter = 2.7 cm. The SANS measurements were carried out at temperatures ranging from 113 to 167 °C.

The SANS profiles from both machines were azimuthally averaged and we report the scattering intensity, I, as a function of q, where $q = 4\pi \sin(\theta/2)/\lambda$ and θ is the scattering angle. The data from the 8 m instrument were converted to absolute scattering intensity as described in paper I. The coherent scattering intensity was obtained after corrections for background, empty cell scattering, detector sensitivity, incoherent scattering, and scattering due to nonuniform deuterium labeling of the homopolymers. The 30 m instrument was used primarily for studying the characteristics of phase-separated samples. The data were corrected for background scattering and detector sensitivity and are reported in relative units.

Light-scattering measurements were conducted on the same samples that were used in the neutron-scattering experiments. The apparatus used for the light-scattering measurements is described in paper I. The total scattered light intensity in the angular range from 2.5° to 10.7° (corresponding to q values ranging from 4.33×10^{-5} to 1.85×10^{-4} Å^{-1}) from a given sample was recorded as a function of time after quenching it from a suitably high temperature in the single-phase regime to selected temperatures.

Theoretical Background

The SANS intensity profiles from multicomponent blends in the single-phase regime were analyzed on the basis of the random phase approximation (RPA). The coherent scattering intensity from an $(n + 1)$ component, incompressible mixture, $I(q)$, is given by eq 1.[2−10]

$$I(q) = \mathbf{B}^{\mathrm{T}}\underline{\underline{S}}(q)\mathbf{B} \qquad (1)$$

A component is defined as a connected chain of identical monomers. The PE/PP/PE−PP blends are thus composed of four components, i.e., $n = 3$. In eq 1, $\mathbf{B}$ is an n dimensional column vector whose elements, B_i, are related to the scattering length density of component i ($B_i = b_i/v_i - b_0/v_0$, where b_i is the scattering length of component i and v_i is the monomer volume of component i). Subscript 0 refers to hPE, the background component. Subscripts 1 and 2 refer to the PE and PP blocks in the PE−PP block copolymer, respectively, and label 3 refers to the PP homopolymer. $\underline{\underline{S}}(q)$ is an n by n structure factor matrix whose elements, S_{ij}, describe correlations between components i and j.

$$S_{ij} = f(\phi_k, N_k, v_k, l_k \chi_{kl}, v; q) \qquad (k, l = 0-3) \qquad (2)$$

where ϕ_k is the volume fraction of component k in the blend, N_k is the number of monomers per chain of component k, l_k is its statistical segment length, v_k is the monomer volume, χ_{kl} is the Flory−Huggins interaction parameter between components k and l, and v is a reference volume, which we set equal to 161.5 Å^3. Expressions for S_{ij} in mixtures of two homopolymers and block copolymer are given in paper I (eqs 2−11).[1] The parameters that are needed to calculate $I(q)$ for a multicomponent PE/PP/PE−PP mixtures were estimated in paper I, and are given in Table 3.

In this paper, we also study scattering from phase-separated blends. In these systems, the scattering profile depends on time, i.e., $I(q,t)$. In simple binary mixtures, evolution of the two-phase structure continues until the phase size is limited by the size of the container. This stage is seldom achieved in polymers due to slow kinetics. One usually observes continuous

Table 3. Parameters Used in RPA Calculations at 148 °C

component					hPE−hPP		dPE−dPP	
param	hPE	dPE	hPP	dPP	hPE	hPP	dPE	dPP
N_i[a]	83	83	178	178	367	376	367	376
v_i (Å^3)	179.0	178.8	174.8	174.6	179.0	174.8	178.8	174.6
l_i (Å)	10.79	10.79	8.61	8.61	12.65	10.10	12.65	10.10
b_i (Å) × 10^4	−0.498	4.952	−0.498	5.156	−0.498	−0.498	6.327	3.784

[a] The numbers of monomer units are based on the C_6H_{12} repeat unit. Interaction parameters at 148 °C, based on a reference volume $v = 161.5$ Å^3 are: $\chi_{hPE/dPP} = 1.39 \times 10^{-2}$, $\chi_{dPE/hPP} = 1.03 \times 10^{-2}$; $\chi_{hPE/hPP} = \chi_{dPE/dPP} = 1.39 \times 10^{-2}$; and $\chi_{hPE/dPE} = 6.43 \times 10^{-3}$, $\chi_{hPP/dPP} = 2.66 \times 10^{-4}$. See paper I[1] for temperature dependence of these parameters.

coarsening, that in turn results in a continuously evolving scattering profile. However, the addition of a surfactant can lead to the formation of thermodynamically stable structures which result in time-independent scattering profiles, i.e., $I(q)$. These structures, which are characterized by periodic concentration profiles, can be of two types: (1) Blends with high surfactant concentrations will form periodic structures with long-range order. These phases can be either crystalline or liquid crystalline, depending on the architecture of the surfactant and the composition of the blend, and they are similar to those found in neat surfactants. In this study, the surfactant is a symmetric diblock copolymer that exhibits an ordered lamellar phase.[1] Although explicit calculations for the particular system that we have studied have not been carried out, we expect that the ordered, multicomponent PE/PP/PE−PP blends with $\phi_{PE}/\phi_{PP} = 1.6$ will have a lamellar structure. (2) Blends with low surfactant concentrations form microemulsions.[11−13] Teubner and Strey[13] showed that the structure within these systems can be described by a two-point, density−density correlation function, $C(r)$, given by

$$C(r) \sim [\exp(-r/\xi)/r] \sin(2\pi r/d) \qquad (3)$$

where r is the distance between the points, d is the average periodicity of the microemulsion, and ξ is the correlation length of the periodic structure. The parameters ξ and d are found to be similar in magnitude due to the lack of long-range order.

The scattering intensity from such a system is given by

$$\frac{1}{I(q)} \sim a + c_2 q^2 + c_4 q^4 \qquad (4)$$

where the coefficients a and c_i are related to d and ξ (details in ref 13).

The applicability of eq 4 to inhomogeneous systems was first demonstrated by Debye and Bueche.[14] In fact, it was shown that the inverse scattering intensity from any inhomogeneous system can be approximated by a power series in q^2, and eq 4 is a truncated version of this equation.[14] In a pioneering publication, Bates et al. used the Teubner−Strey approach to study the thermodynamic properties of a multicomponent mixture of two homopolymers and a block copolymer.[15] They identified the temperature and composition at which the coefficients a and c_2 tend to zero. This is a signature of the Lifshitz point, which is the terminus of the Lifshitz line.[15,16]

SANS from Multicomponent Mixtures

The q dependence of the coherent SANS intensity, I, from the BH series at selected temperatures is shown in Figure 2. The PP homopolymer is the only labeled species in this series of blends. The scattering contrast between the components of hPE−hPP block copolymer (components 1 and 2) and the background component, hPE (component 0), is negligible. This implies that $B_2 \approx B_1 = 0$ but $B_3 \neq 0$ (see Table 3). Substituting these values in eq 1, we get,

$$I(q) \approx B_3^2 S_{33}(q) \qquad \text{(BH series)} \qquad (5)$$

The scattering profiles in Figure 2 are therefore related to the distribution of the segments of the PP chains in the multicomponent mixtures.

The scattering profiles from samples BH05, BH10, and BH20 are monotonic functions of q, as shown in Figures 2a−c. This suggests that the distribution of homopolymer segments in these multicomponent blends is similar to that in simple, binary mixtures. The scattering profiles from sample BH30, shown in Figure 2d, are also monotonic functions of q at temperatures above 148 °C. However, a weak scattering peak at $q = 0.01$ Å^{-1} appears at temperatures below 148 °C. This indicates the formation of a periodic structure with a length scale of 630 Å ($2\pi/q_{peak}$, where q_{peak} is the value of q at the scattering peak). The peak is, however, very close to the beam stop and therefore not clearly resolved. In Figures 2e,f we show SANS data obtained from samples BH50 and BH75. In these samples, decreasing temperature results in the development of a well-defined scattering peak at $q \approx 0.014$ Å^{-1}, and the scattering intensity at the lowest accessible q ($q = 0.007$ Å^{-1}) is strongly suppressed.

The q dependence of the coherent SANS intensity, I, from the BB series at selected temperatures is shown in Figure 3. These blends contain two deuterium-labeled components, namely the dPE and dPP blocks of the block copolymer. This implies that $B_3 = 0$, and B_1 and B_2 are nonzero (see Table 3). Substituting these values into eq 1 gives

$$I(q) \approx B_1^2 S_{11}(q) + 2B_1 B_2 S_{12}(q) + B_2^2 S_{22}(q) \qquad \text{(BB series)} \qquad (6)$$

The SANS profiles from BB blends are thus related to distribution of dPE and dPP segments of the block copolymer (S_{11}) and (S_{22}), as well as interblock correlations (S_{12}). The data obtained from the BB series are therefore complimentary to that obtained from the BH series. The SANS profiles from a melt of pure dPE−dPP block copolymer exhibited a well-defined scattering peak at $q = 0.016$ Å^{-1} at all accessible temperatures; see Figure 12 in paper I. This is due to correlations between the dPE and dPP blocks. In theory, these correlations persist at arbitrarily high (infinite) temperatures due to the connectivity of the blocks.[2,3] Consequently, the scattering profiles from block copolymers are always peaked at a finite scattering angle.

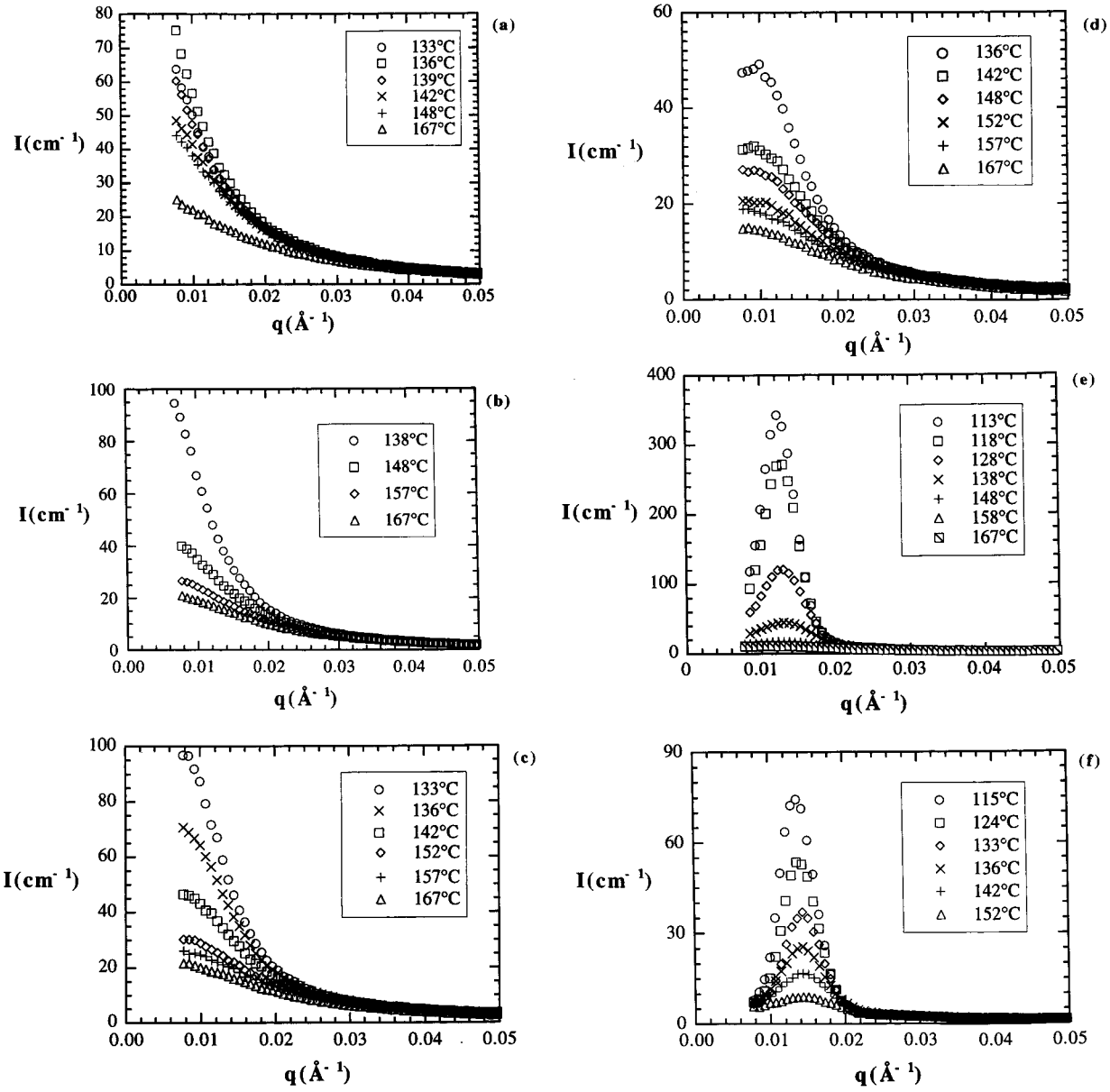

Figure 2. Coherent SANS intensity profiles obtained from the BH series (hPE/dPP/hPE−hPP mixtures) with $\phi_{hPE}/\phi_{dPP} = 1.6$ at selected temperatures: (a) blend BH05 (5% block copolymer); (b) BH10; (c) BH20; (d) BH30; (e) BH50; (f) BH75.

Equation 6 applies to a pure block copolymer melt with the additional constraint that $S_{11}(q) = S_{22}(q) = -S_{12}(q)$, due to incompressibility. The peak in the scattering profiles is due to the fact that function S_{11} (and S_{22}) contains a minimum ("hole") at finite q, regardless of temperature. The scattering peaks at high temperatures is sometimes called the "correlation hole" effect.[2]

The SANS profiles from samples BB05 and BB10 are shown in Figure 3a,b. The scattering profiles are monotonic functions of q in the accessible temperature range, 114−167 °C. Correlations due to the connectivity of the dPE and dPP blocks in the copolymer are present in these multicomponent blends, i.e., function S_{11} contains a minimum at finite q. However, $S_{11}(q) \neq S_{22}(q) \neq -S_{12}(q)$, and the hole in S_{11} may therefore not be evident in the scattering profiles. In the case of BB05 and BB10, the correlation hole is washed out due to the overwhelming presence of the PE and PP homopolymers. The scattering profiles from both BH and BB blends are thus monotonic functions of q when the volume fraction of block copolymer is less than 0.1. There is however, an important difference when these sets of data are compared. The scattering data from the BH samples (Figures 2a,b) exhibited a strong temperature dependence, while the data from the BB samples (Figures 3a,b) are virtually independent of temperature.

The temperature dependence of the scattering profiles from sample BB20 is shown in Figure 3c. A discernible increase in the scattering intensity at $q < 0.02$ Å^{-1} was observed at low temperatures. It is evident that the distribution of block copolymer segments becomes sensitive to temperature when the block copolymer volume fraction is increased from 0.10 to 0.20. The temperature dependence of the scattering profiles from sample BB30 is shown in Figure 3d. At temperatures ≤121 °C we see the emergence of a scattering peak at $q = 0.01$ Å^{-1}, implying the presence of a periodic structure. In Figure 3e,f, we show data from BB50 and BB75, wherein well-defined scattering peaks are evident over most of the accessible temperature range.

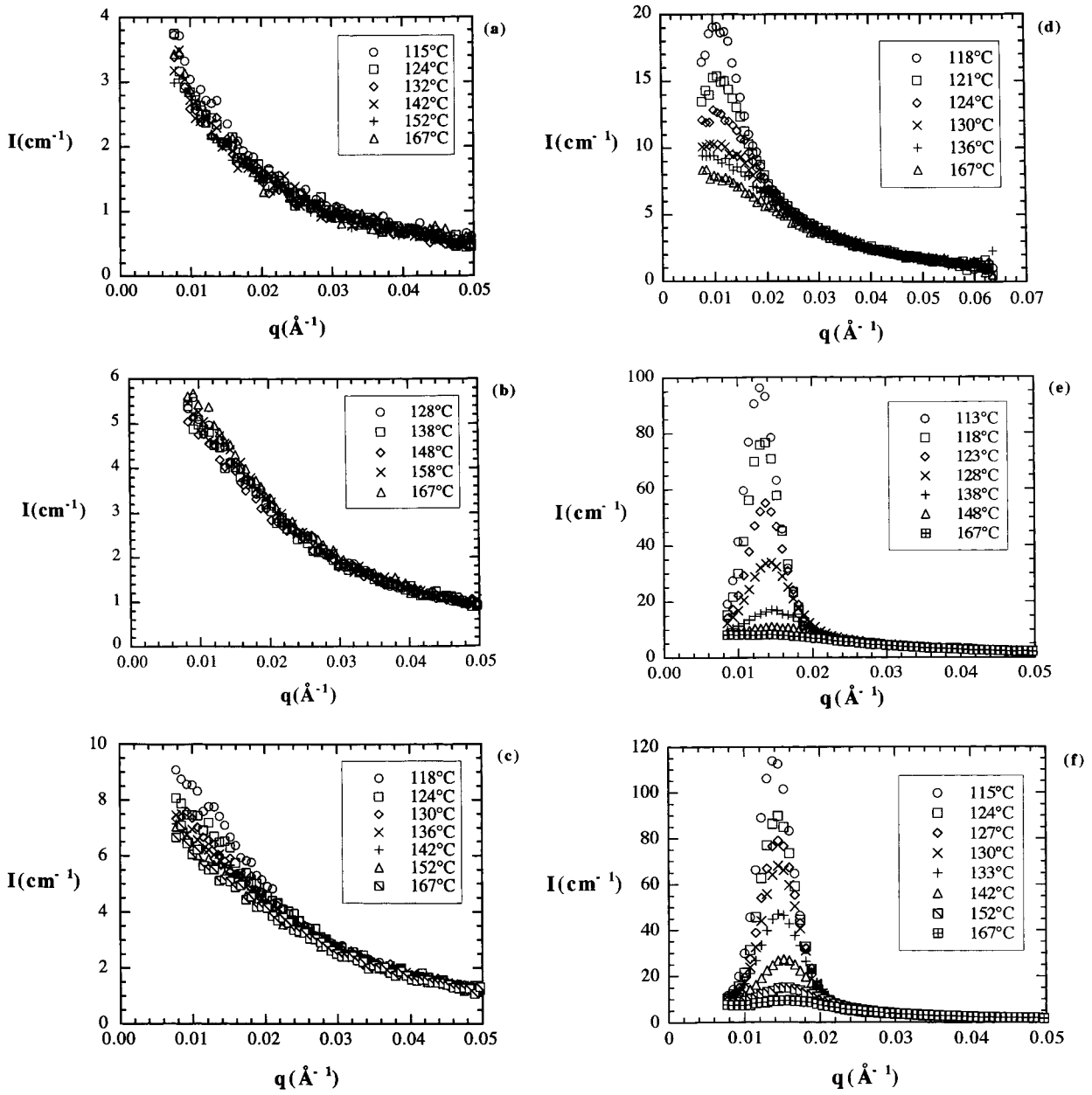

Figure 3. Coherent SANS intensity profiles obtained from the BB series (hPE/hPP/dPE−dPP mixtures) with $\phi_{hPE}/\phi_{hPP} = 1.6$ at selected temperatures: (a) blend BB05 (5% block copolymer); (b) BB10; (c) BB20; (d) BB30; (e) BB50; (f) BB75.

The qualitative features of the scattering profiles of the BB series at block copolymer volume fractions greater than or equal to 0.3, are remarkably similar to those obtained from BH series in the same concentration range (compare Figure 2d−f with Figure 3d−f, respectively). This implies that the distribution of the PP homopolymer chains, measured in the BH series, is strongly coupled to the distribution of the PE and PP blocks of the copolymer, measured in the BB series, when $\phi_{PE-PP} \geq 0.3$. On the other hand, when $\phi_{PE-PP} \leq 0.1$, the results from the BH series and the BB series are dramatically different. Experiments on the BB series yield scattering profiles that are nearly independent of temperature, while experiments on the BH series yield scattering profiles that are strongly temperature dependent (compare Figure 2a,b with Figure 3a,b). This implies that the distribution of the PP homopolymer chains measured in the BH series experiments, are not coupled to the distribution of the PE and PP segments of the copolymer chains when $\phi_{PE-PP} \leq 0.1$. The blend with $\phi_{PE-PP} = 0.2$ lies at the crossover between coupled and uncoupled behavior.

Concentration Fluctuations Prior to Macrophase Separation

When the volume fraction of block copolymer is 0.1 or lower, the measured SANS profiles from both BH and BB blends are devoid of scattering peaks. This is characteristic of systems approaching macrophase separation. Samples BH10 and BB10 are representative of such systems. In Figure 4, we present SANS data from BH10 at temperatures where the sample is single-phase; the determination of the phase boundary in these multicomponent systems will be described in a subsequent section. The solid curves in Figure 4 represent calculated scattering profiles based on the RPA. The parameters used in these calculations, which are based on the results on binary PE/PP blends and the pure PE−PP block copolymer reported in paper I, are summarized in Table 3. The value of $\chi_{hPE/hPP}$ was adjusted to

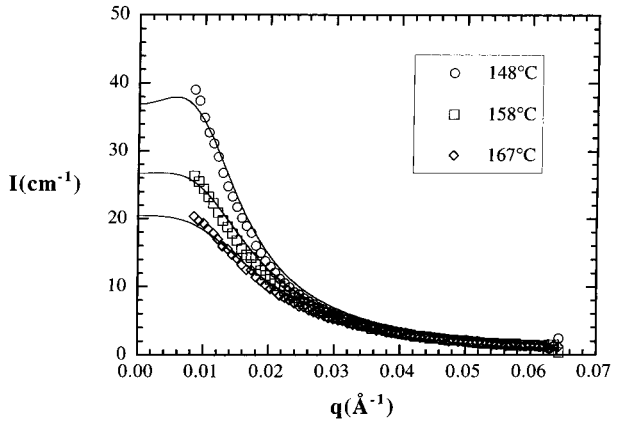

Figure 4. Coherent SANS intensity profiles from a blend of hPE/dPP/hPE−hPP with $\phi_{hPE}/\phi_{dPP} = 1.6$ and $\phi_{hPE-hPP} = 0.1$ (BH10) at selected temperatures. The solid curves through the data are RPA calculations with $\chi_{hPE/hPP}$ as the adjustable parameter.

minimize the sum of the square of the deviations between theory and experiment. (The quantity $\Delta\chi$, defined as the difference between the right-hand sides of eqs 16 and 17 in paper I, was kept constant in this fitting procedure; see paper I.) It is evident that the RPA-based theory with one adjustable parameter is in quantitative agreement with experiments on BH10.

It is generally believed that the statistical segment lengths of a chain of monomers should be independent of molecular architecture. In contrast, the experimental results reported in paper I[1] indicate a substantial difference in statistical segment lengths of PE and PP, depending on whether the monomers were parts of homopolymer or copolymer chains. The SANS experiments on binary PE/PP blends yielded statistical segment lengths that were about 20% smaller that those measured from experiments on the pure PE−PP block copolymer. This causes no difficulty in the application of multicomponent RPA because the statistical segment length of each component can be specified separately. In the case of sample BH10, quantitative agreement between theory and experiment is found without adjusting the statistical segment lengths. This suggests that the polymer chains in the ternary blend are unperturbed, relative to their state in the binary PE/PP blend and the pure PE−PP block copolymer.

The scattering intensity from multicomponent blends arises due to correlations between the labeled monomers in the blend, which can be either intramolecular or intermolecular in origin. In the BH series only homopolymer PP is labeled. In this case, intramolecular correlations arise due to connectivity of the monomers in the PP chains, while intermolecular correlations arise due to interactions between the components of the blend. At infinite temperature (i.e., $\chi_{ij} = 0$ for all i and j), the distribution of PP chains is expected to be perfectly random, subject to the constraints of excluded volume, which lead to near incompressibility. Under these conditions, correlations between PP segments arise only due to the connectivity of the PP chains and excluded volume. As temperature is decreased, incipient macrophase separation is announced by large-length-scale concentration fluctuations, which, in turn, lead to an increase in low-angle scattering. To focus on the large-length-scale concentration fluctuations, we define an excess scattering intensity, $I_{EX}(q)$ as follows:

$$I_{EX}(q) = I(q) - I_{CONN}(q) \tag{7}$$

where the connectivity contribution, $I_{CONN}(q)$, is computed from multicomponent RPA (eqs 1 and 2) with all χ_{ij} set to zero.

$$I_{CONN}(q) = \mathbf{B}^T \underline{\underline{S}}(\phi_k, N_k, v_k, l_k \chi_{kl} = 0, v; q)\mathbf{B} \tag{8}$$

The q dependence of I_{EX} at selected temperatures for BH10 is shown in Figure 5. Significant excess scattering is evident at $q < 0.025$ Å^{-1} at all temperatures. This indicates an amplification of homopolymer concentration fluctuations with length scales greater than 250 Å [$2\pi/(q = 0.025$ Å$^{-1})$].

In Figure 5, we also show the q dependence of I_{EX} measured in sample BB10. In the BB series, the labeled species is the dPE−dPP block copolymer. We see that I_{EX} from sample BB10 is nearly zero at all accessible q and at all temperatures. This indicates that the distribution of PE−PP chains in BB10 is perfectly random, and the measured scattering from BB10 is entirely due to the connectivity of the monomers in the PE−PP chains. In addition, the measured scattering profiles are consistent with RPA predictions with all $\chi_{ij} = 0$. The RPA calculations of $I(q)$ for sample BB10 are thus independent of χ_{ij}. In this case, minimizing the sum of the square of the deviations between theory and experiment by adjusting $\chi_{hPE/hPP}$ is not fruitful.

Concentration Fluctuations Prior to Microphase Separation

When the volume fraction of block copolymer is greater than 0.3, the measured scattering profiles from both BH and BB blends have well-defined peaks at finite scattering angles. This behavior is typical of systems that exhibit microphase separation. Samples BH50 and BB50 are representative of such systems. In Figure 6 we compare experimental data (symbols) from BH50 with theoretical fits based on the RPA (solid curves). We have restricted our attention to high temperatures where the samples are single-phase; the determination of the phase boundary in these blends will be described in a subsequent section. The fitting procedure used for BH50 was identical to that used for fitting the BH10 data, and involves one adjustable parameter, $\chi_{hPE/hPP}$. It is evident that this adjustment leads to quantitative agreement between theory and experiment (Figure 6).

To focus on the intermolecular correlations of the PP homopolymer, we computed I_{EX} for BH50 using eqs 7 and 8. The results are shown in Figure 7 where we plot I_{EX} versus q at selected temperatures. A well-defined peak at $q = 0.013$ Å^{-1} is evident in $I_{EX}(q)$ of BH50 at 148 °C. This indicates a periodic arrangement of the dPP homopolymer chains with a length scale of about 490 Å. The peak grows with decreasing temperature, implying an increase in the amplitude of the periodic structure. However, $I_{EX}(q)$ in the limit of low q also increases with decreasing temperature. At the lowest accessible q ($q = 0.008$ Å^{-1}), the value of I_{EX} increases by about a factor of 3 in the accessible temperature range. This indicates the increasing presence of intermolecular aggregates with large-length-scales (>780 Å) with decreasing temperature.

In Figure 8, we plot the q dependence of I at selected temperatures from blend BB50. The solid lines in Figure 8 are RPA fits with $\chi_{hPE/hPP}$ as the only adjustable parameter. We find that the agreement between theory

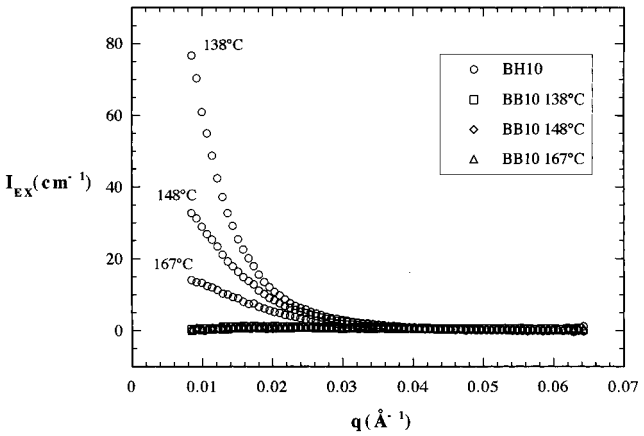

Figure 5. Excess scattering intensity, $I_{EX}(q)$, from BH10 (hPE/dPP/hPE−hPP) and BB10 (hPE/hPP/dPE−dPP) at selected temperatures. Both blends contain 10% diblock copolymer.

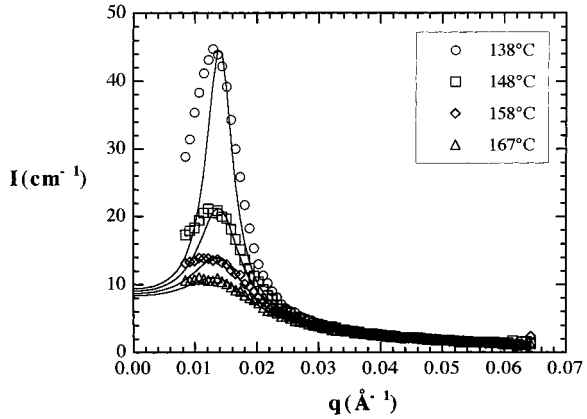

Figure 6. Coherent SANS intensity profiles from a blend of hPE/dPP/hPE−hPP with $\phi_{hPE}/\phi_{dPP} = 1.6$ and $\phi_{hPE-hPP} = 0.5$ (BH50) at selected temperatures. The solid curves through the data are RPA calculations with $\chi_{hPE/hPP}$ as the adjustable parameter.

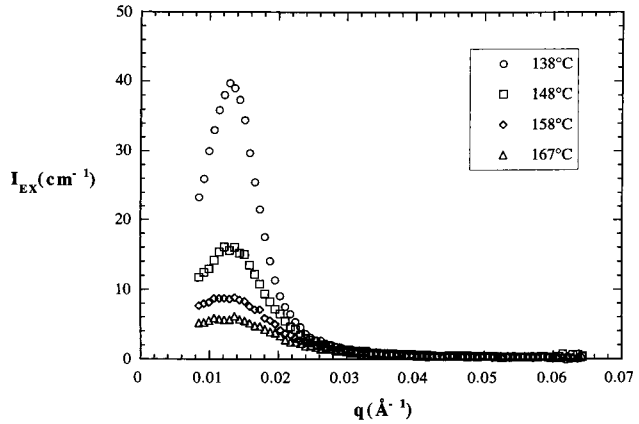

Figure 7. Excess scattering intensity, $I_{EX}(q)$, from BH50 (hPE/dPP/hPE−hPP) at selected temperatures.

and experiment is reasonable. The agreement between theory and experiment in the high q regime is not as good as that observed in the BH50 blend. This suggests that the conformations of the block copolymer chains in the multicomponent blends are different from those found in the pure dPE−dPP melt. The RPA does not provide any information about the origin of these conformational changes.

In Figure 9, we plot the q dependence of I_{EX} for the BB50 blend. These data show a well-defined peak at q

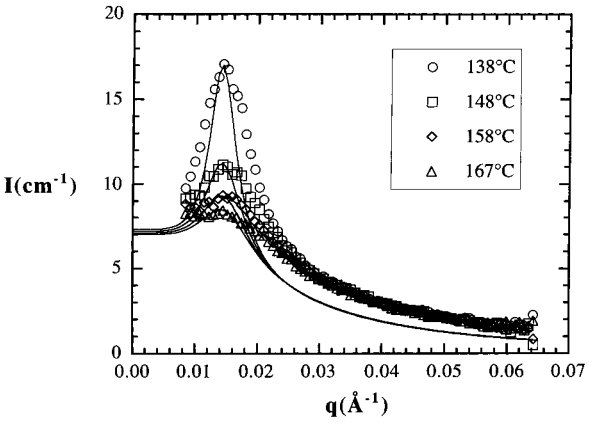

Figure 8. Coherent SANS intensity profiles from a blend of hPE/hPP/dPE−dPP with $\phi_{hPE}/\phi_{hPP} = 1.6$ and $\phi_{dPE-dPP} = 0.5$ (BH50) at selected temperatures. The solid curves through the data are RPA calculations with $\chi_{hPE/hPP}$ as the adjustable parameter.

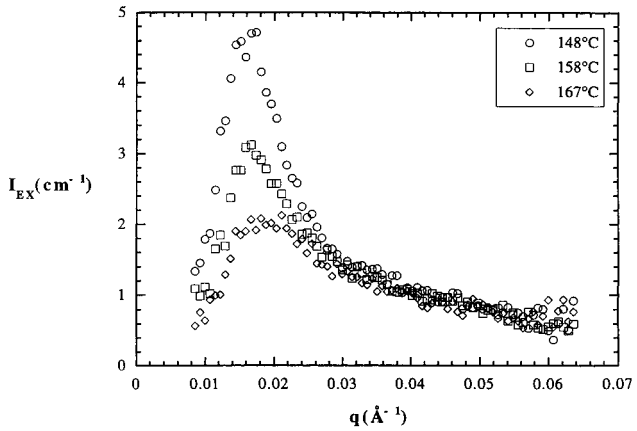

Figure 9. Excess scattering intensity, $I_{EX}(q)$, from blend BB50 (hPE/hPP/dPE−dPP) at selected temperatures.

$= 0.014$ Å^{-1}, which is similar in some respects to the q dependence of I_{EX} of blend BH50. Careful comparison of Figure 9 with Figure 7, however, reveals a major difference between the q dependence of I_{EX} of samples BH50 and BB50. In BB50, I_{EX} approaches zero as $q \rightarrow 0$, while in BH50, I_{EX} is finite as $q \rightarrow 0$. We thus see evidence for purely periodic concentration fluctuations and the absence of large-length-scale fluctuations in BB50. If there were any form of intermolecular aggregation of the PE−PP block copolymer chains such as micelle formation, then I_{EX} would be finite in the forward direction. In fact, finite polydispersity, which is always present in anionically synthesized block copolymers, also leads to a finite I_{EX} in the forward direction.[17] The fact that the measured $I_{EX}(q)$ in BB50 approaches zero at low q is a direct indication that polydispersity in either composition or molecular weight has no measurable effect on the thermodynamics. Note that the low-q scattering prior to subtraction of I_{CONN} is finite (Figure 8). The true intramolecular nature of the segregation of the blocks becomes evident only after the connectivity contribution was subtracted (Figure 9).

Estimation of χ in Multicomponent Systems

In Figure 10, we show the temperature dependence of $\chi_{hPE/hPP}$ in blends BH10, BH50, and BB50, obtained by fitting SANS data to the RPA based theory (see previous section). Also shown in this figure are the χ

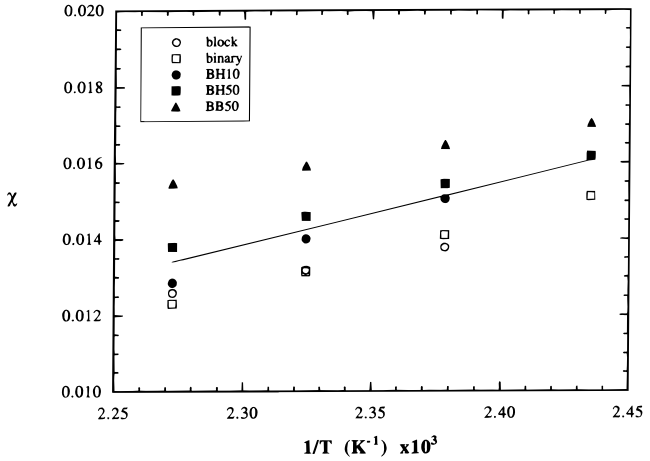

Figure 10. χ parameter between hPE and hPP chains: BH10 (filled circles); BH50 (filled squares); BB50 (filled triangles); dPE−dPP block copolymer after fluctuation corrections (open circles), binary PE/PP blends (open squares).

parameters obtained in the binary PE/PP blends and the dPE−dPP block copolymer after fluctuation corrections (see paper I).[1] The following straight line was obtained by linear regression using all the data in Figure 10:

$$\chi_{\mathrm{hPE/hPP}} = 16.63/T - 2.45 \times 10^{-2} \quad (v = 161.5\ \text{Å}^3) \quad (9)$$

At the lowest temperature (138 °C), the deviation between the experimentally determined χ parameters and eq 9 is 5% or less. Estimated uncertainties in the determination of χ, due mainly to errors in polymer characterization and calibration of the SANS machine, are about 10%.[10] The observed scatter in the experimentally determined χ parameter at low temperatures is thus within experimental error. Note that the characteristics of the two-component and multicomponent systems that are included in Figure 10 differ widely from each other. The fact that the variety of scattering profiles observed in these systems are consistent with a single, composition independent χ parameter lends considerable support to the random phase approximation. At higher temperatures, the agreement between the χ parameters measured in BH10 and BH50 are in reasonable agreement with the measurements in the two-component systems (see Figure 10). However, significant deviations are seen the BB50 blend data, especially at the high temperatures. At the highest temperature (167 °C), the deviation between the BB50 χ parameter and eq 9 is 25%. This may be due to fluctuation effects that are not included in the RPA-based theories. Recall that the χ parameters measured in the PE/PP blends were in agreement with those obtained from the dPE−dPP melt, only after fluctuation corrections were incorporated in the analysis of the dPE−dPP data.[1]

Liquid−Liquid Phase Separation in Multicomponent Blends

The SANS data from BH10 discussed thus far were restricted to temperatures greater than 138 °C. In Figure 11a, we show $I(q)$ over the entire temperature range for BH10. It is evident that the high-q data obtained at temperatures >128 °C are nearly superposable. However, the high-q data obtained at 113 and 118 °C show significant deviations. The distinction between

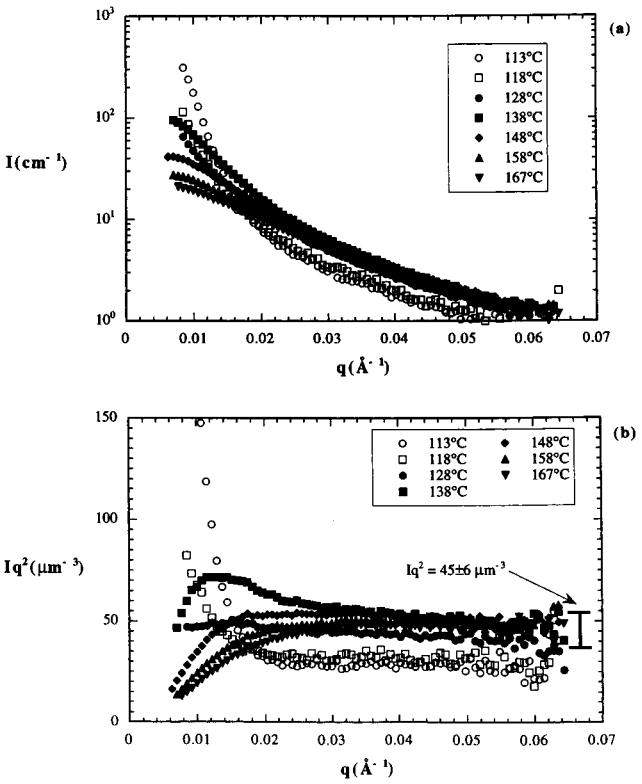

Figure 11. (a) Coherent SANS intensity profiles, I versus q, from BH10 (10% block copolymer). (b) Kratky plots, Iq^2 versus q from BH10. The value of the Kratky plateau, predicted by RPA calculations, is shown with estimated uncertainty.

the scattering profiles in the high-q regime can be seen more clearly in Figure 11b where we plot the data Iq^2 versus q (Kratky format). It is evident that Iq^2 approaches a plateau at high q. The RPA-based value for the Kratky plateau, which was calculated using eqs 1 and 2 with the parameters given in Table 3, is also shown in Figure 11b. The value of the Kratky plateau in multicomponent blends depends only on the statistical segment lengths, monomer volumes, and monomer scattering lengths, which are either weak functions of temperature or independent of temperature. The experimental Kratky plateaus at temperatures greater than 128 °C are nearly temperature independent, and in good agreement with the theoretical prediction. A slight decrease from the high-temperature Kratky plateau is evident at 128 °C. At 118 and 113 °C, we see clear departures from the high-temperature Kratky plateau. This is a well-documented signature of macrophase separation in binary[18] and multicomponent[19] polymer blends. We conclude that BH10 is macrophase-separated at temperatures below 128 °C.

The results of light-scattering experiments obtained from BH10 are shown in Figure 12. The blend was equilibrated at 180 °C for 4 h and then quenched to a series of temperatures. The time dependence of the scattering signal, normalized by the signal prior to the quench, is shown in Figure 12. When the sample was quenched to 146 °C, we found no increase in the light-scattering signal. However, quenching the sample to 142 °C results in a monotonic increase in the scattered light, indicating the onset of liquid−liquid phase separation. Quenching to 144 °C results in an initial increase in the light-scattering signal, but after 200 min, the signal reaches a time independent plateau. This is

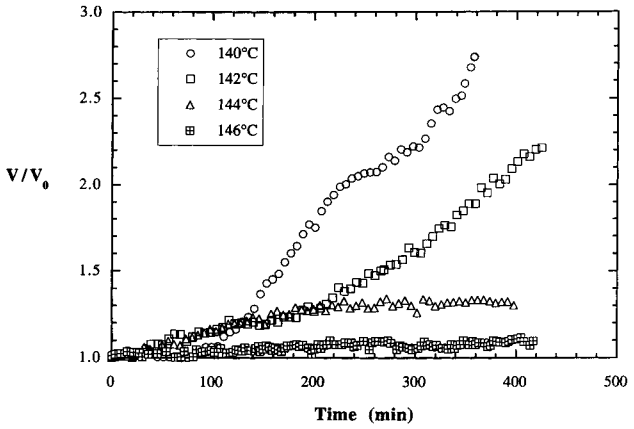

Figure 12. Time dependence of the normalized light-scattering intensity from BH10 (10% block copolymer) after the sample was quenched from 180 °C to several temperatures, as indicated. V is the signal from the photodetector, and V_0 is the signal at $t = 0$. Evidence for macrophase separation is seen at temperatures ≤142 °C.

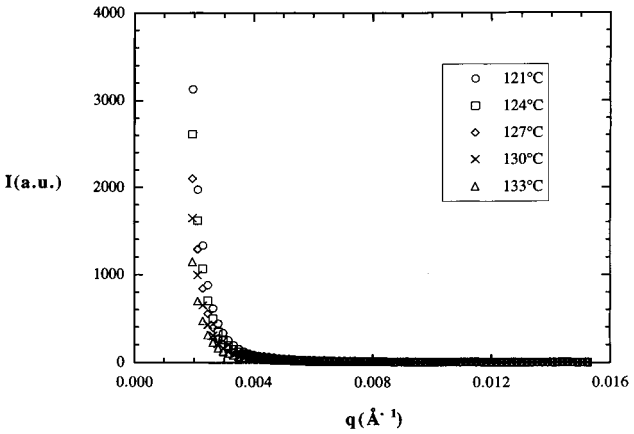

Figure 13. Neutron-scattering profiles at selected temperatures from BH10 (10% block copolymer) in the low-q range, obtained using the 30 m SANS machine.

not typical of systems undergoing simple liquid−liquid phase-separation. One possibility is that the later stages of coarsening of the phase-separated structure are much slower (or arrested) by the presence of the block copolymer. However, in BH10, this behavior is only observed over a narrow temperature range. Since a monotonic increase in light-scattering signal is an unambiguous signal of liquid−liquid phase separation, we conclude that liquid−liquid phase separation in BH10 occurs at 143 ± 1 °C, acknowledging the possibility of more complex phenomena in the vicinity of the transition temperature. Note that this is somewhat higher than the phase separation temperature deduced from neutron scattering, which was 128 ± 10 °C. Due to limited access to the neutron beam, the SANS data from sample BH10 reported in Figure 11 were acquired after equilibrating the sample at each temperature for about 1 h. Perhaps, if we had used longer equilibration times, the SANS data at 138 °C would have exhibited signatures of liquid−liquid phase separation.

To confirm our conclusion regarding macrophase separation in BH10, we used the 30 m SANS machine to access $q < 0.007$ Å^{-1}. The sample was annealed at 170 °C and studied as a function of decreasing temperature. The scattering profiles, shown in Figure 13, are monotonic functions of q. This confirms the lack of

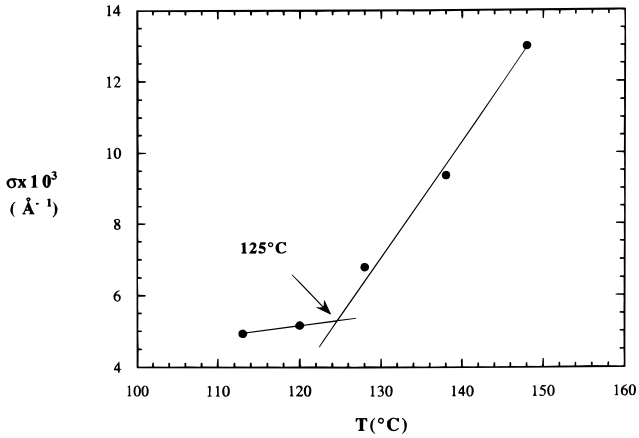

Figure 14. Temperature dependence of the peak width, σ, obtained from BH50 (50% block copolymer). Evidence for order formation is seen at temperatures below 125 °C.

periodic structures in BH10 and that it exhibits macrophase separation.

Order Formation in Multicomponent Blends

In paper I, we used two methods to determine the order-to-disorder transition temperature in the pure dPE−dPP block copolymer.[1] In the first method, we produced a nonrandom distribution of lamellae by perturbing the sample and identified the transition temperature as the point at which the scattering profiles became isotropic. In the second method, we examined the sample without perturbing it, and the transition temperature was identified as the point at which an abrupt change in the peak width was noted. Both methods gave identical results for the transition temperature. Since the first method relies on the response of the ordered structures to external fields and since little is known about the effect of external fields on multicomponent systems, we chose to apply the second method to determine the transition temperature of BH50. The scattering profiles at each temperature from BH50 (Figure 2 e), in the vicinity of the peak, were fit to a Gaussian function $I(q) = I_0 \exp\{-2(q - q_{peak})^2/\sigma^2\}$. The temperature dependence of the peak width, σ, is shown in Figure 14. We see an abrupt change in the temperature dependence of σ in the vicinity of 125 °C. On this basis, we conclude that the order-to-disorder transition temperature of BH50 is 125 ± 5 °C. We also studied the changes in the light-scattering signal after quenching BH50 from 170 °C to several temperatures between 120 and 140 °C range. No detectable changes in the light-scattering intensity were found, indicating the lack of large-scale structures in BH50. This confirms our conclusion that this sample exhibits an order-to-disorder transition at 125 °C.

Formation of Micoremulsions

In Figure 15 a, we show the evolution of SANS profiles after quenching sample BH20 from 170 to 114 °C. These data were acquired on the 30 m machine. Time zero is defined as the time at which the quench was initiated and it took about 10 min for the sample temperature to reach 114 °C. The development of a well-defined scattering peak is evident in Figure 15a. The scattering profiles obtained at $t = 81$ min and $t = 840$ min are nearly superposable. The time-independence of the scattering profiles and the presence of the

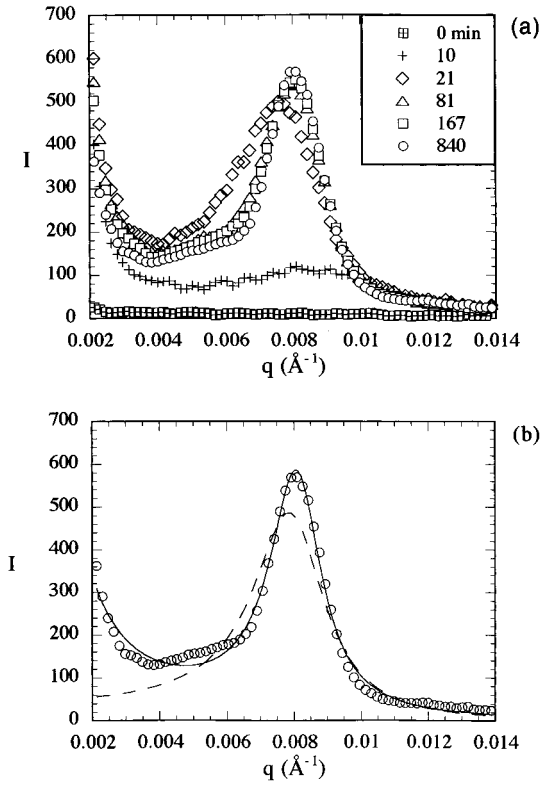

Figure 15. (a) Time dependence of SANS profiles from BH20 after a quench from 170 to 114 °C. (b) Least-squares fits of the 840 min data in (a): (dashed curve) eq 4; (solid curve) eq 11.

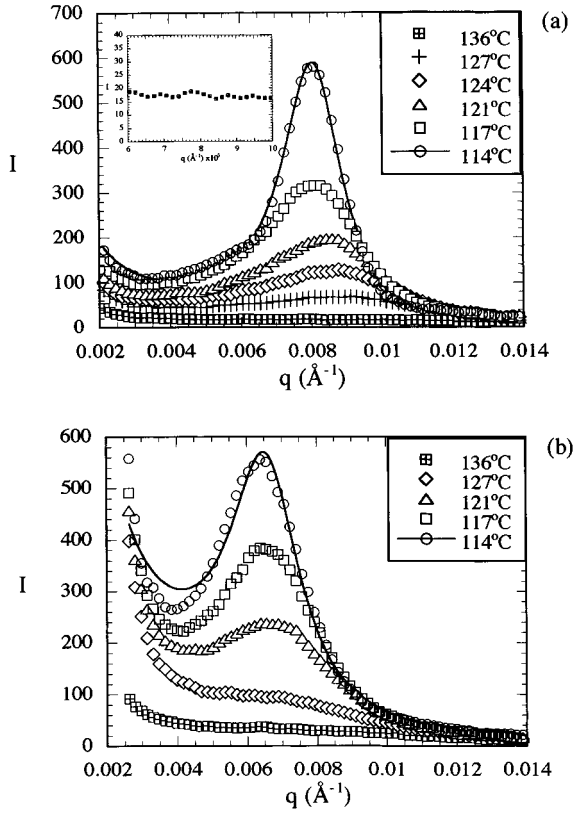

Figure 16. Temperature dependence of SANS profiles from (a) BH20, and (b) BH15 after equilibrating the sample at each temperature for about 1 h. The inset in (a) shows the 136 °C data on an expanded scale. Solid curves represent least-squares fits of eq 11 through the 114 °C data.

scattering peak are necessary conditions for the formation of stable, periodic structures. The scattering peak in BH20 is outside the q-range of the 8 m SANS machine and was therefore not evident in the BH20 data shown in Figure 2c.

In some respects, the scattering profiles shown in Figure 15a are similar to those found in oil/water/surfactant microemulsions.[13] In these small molecule systems, the enrichment of the surfactant molecules at the internal interfaces leads to the formation of weakly ordered, periodic structures. The scattering profiles from a variety of microemulsions contain a single broad scattering peak, which are in quantitative agreement with the Teubner−Strey model (eq 4). In Figure 15b, we compare the experimental data from BH20 with the Teubner−Strey model. The dashed curve represents the least-squares fit of the data to eq 4. The lack of agreement between the experiments and theory is obvious. In addition to a scattering maximum, the data from the PE/PP/PE−PP blends exhibit scattering minima in the vicinity of $q = 0.004$ Å^{-1}, which is inconsistent with eq 4. It should be noted that similar scattering profiles have been observed in oil/water microemulsions.[20]

We propose that the correlations in PE/PP/PE−PP microemulsions are described by a simple extension of the Teubner−Strey correlation function,

$$C(r) \sim [\exp(-r/\xi)/r][\alpha + \sin(2\pi r/d)] \qquad (10)$$

where large-scale, disordered structures with Ornstein−Zernike correlations coexist with a periodic, microemulsion. We refer to the disordered structures as emulsification defects. The numerical value of α, relative to unity, is a measure of defect density. The model is highly simplified because it assumes that the defects and the periodic structure can be described by a single correlation length, ξ.

The intensity profile[14] that corresponds to the correlation function (eq 10) is given by

$$I(q) \sim \frac{\alpha\xi^2}{1 + q^2\xi^2} + \frac{4\pi d^3\xi^3}{(16\pi^4\xi^4 + 8\pi^2 d^2\xi^2 + d^4) + (2d^4 - 8d^2\pi^2\xi^4)q^2 + \xi^4 d^4 q^4} \qquad (11)$$

The solid curve in Figure 15b show the best fit to eq 11. It is evident that despite its simplicity, the proposed model captures the essential features of the data. The parameters used to obtain the fit are $d = 780$ Å, $\xi = 1080$ Å, and $\alpha = 0.17$. Like small molecule microemulsions, d and ξ are comparable, due to the lack of long-range order.[13]

To determine the onset of microemulsion formation in BH20, the SANS profiles from the sample were recorded as a function of decreasing temperature. The sample was first annealed at 170 °C and then cooled in steps. The scattering profiles were acquired after the sample was equilibrated at each temperature for about 70 min. The results of these experiments are shown in Figure 16 a. It is evident that the scattering profiles obtained at temperatures below 124 °C contain a well-defined scattering peak while those obtained above 136 °C were devoid of scattering peaks. This indicates that the formation of modulated phases occurs at 131 ± 6

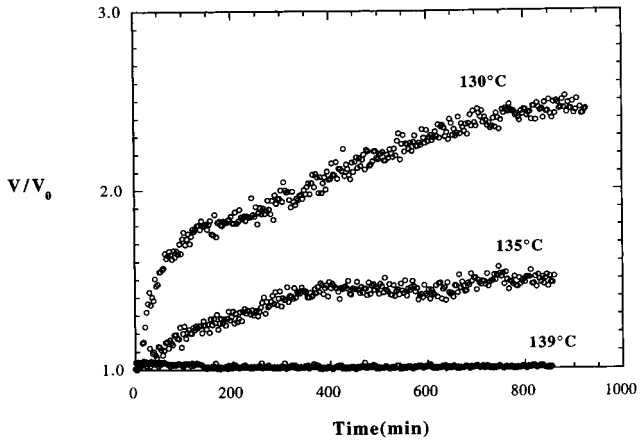

Figure 17. Time dependence of the normalized light-scattering intensity from BH20 (20% block copolymer) after the sample was quenched from 160 °C to several temperatures, as indicated. V is the signal from the photodetector, and V_0 is the signal at $t = 0$.

°C. However, the scattering peaks in BH20 are accompanied by an upturn in the low-angle scattering (Figure 16 a). We therefore use eq 11 to analyze the data. The solid line is the best least-squares fit of the 114 °C data to eq 11. The parameters used to obtain the fit are $d = 780$ Å, $\xi = 1009$ Å, and $\alpha = 0.08$. By comparing these results with the parameters obtained after a rapid quench to 114 °C given in the previous paragraph, we see that the periodicity of the emulsified structure (d) is unaffected by thermal history and may therefore be considered to be an equilibrium property. On the other hand, the characteristics of the defects (ξ and α) depend on thermal history and are therefore nonequilibrium properties of the blend.

In Figure 16b we show the SANS profiles obtained from BH15 as a function of decreasing temperature. The thermal history used for obtaining these data was identical to that used to obtain the data in Figure 16a. The scattering profiles from the BH15 sample are also consistent with eq 11; the solid curve represents the best fit through the data at 114 °C with $d = 948$ Å, $\xi = 840$ Å, and $\alpha = 0.35$. The main difference between BH15 and BH20 is that the length scale of the periodicity in the microemulsion and the defect density are larger in BH15 than in BH20.

The light scattering results obtained from BH20 are shown in Figure 17. A monotonic increase in the light-scattering intensity was observed when the sample was quenched to 130 °C (or lower), indicating the onset of macrophase separation. However, the SANS data indicate the presence of a scattering peak at temperatures below 127 °C (see Figure 16a). We, thus, see that sample BH20 exhibits characteristics of both microphase as well as macrophase separation. Note the consistency in the SALS and the SANS data; the large-scale structures that cause an upturn in the low-q SANS profiles (Figure 15a) are also detected by light scattering (Figure 17). On the basis of the neutron- and light-scattering results, we conclude that BH20 exhibits a liquid-to-microemulsion transition at 130 ± 5 °C. The SANS profiles obtained on the 30 m machine (Figure 16a, inset), at temperatures ≥135 °C, do not contain scattering peaks. The formation of the weakly ordered microemulsion in BH20 is therefore not announced by a pretransitional scattering peak.

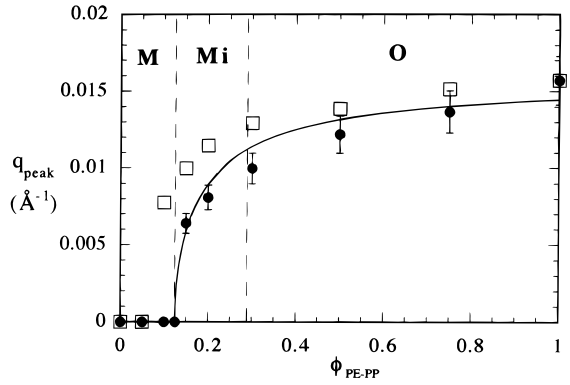

Figure 18. Experimentally determined dependence of q_{peak} on block copolymer volume fraction, ϕ_{PE-PP} (BH series), represented by filled circles. The bars represent the range of q_{peak} values that were obtained in the temperature range where scattering peaks were observed. The solid curve is a least-squares fit of the experimental data (filled circles) to eq 12. The RPA predictions for q_{peak} versus ϕ_{PE-PP} in the single-phase region, given in paper I,[1] are represented by open squares. Macrophase-separated systems (M), microemulsions (Mi), and ordered phases (O) are identified, as described in the text.

Phase Diagram of PE/PP/PE−PP Blends

In Figure 18 we plot the dependence of the q_{peak} measured from the BH series on block copolymer concentration (ϕ_{PE-PP}). The bars in Figure 18 show the range of q_{peak} values measured at different temperatures from a given sample in both single-phase as well as phase-separated regimes. For $\phi_{PE-PP} < 0.15$, the scattering maxima are in the forward direction, i.e., $q_{peak} = 0$. Increasing the block copolymer concentration from 0.15 to 1.0 results in a continuous increase in q_{peak}. Also shown in Figure 18 are the results of RPA calculations of q_{peak} for the BH series, at temperatures just above the phase transition temperatures.[1] It is evident that there is reasonable agreement between the experimental data and the theoretical predictions.

Gompper and Schick[12] have proposed the following equation for the dependence of q_{peak} on surfactant concentration:

$$q_{peak}R = \cos^{-1}\left(\frac{\phi_c}{\phi_{PE-PP}}\right) \qquad (12)$$

where R is a measure of molecular size of the surfactant, and ϕ_c is the critical surfactant concentration required for obtaining modulated phases. The solid curve in Figure 18 is the least-squares fit of eq 12 through the experimental data for samples that contained a periodic structure, i.e., $\phi_{PE-PP} \geq 0.15$. Our estimates for constants in eq 12 are $R = 103$ Å and $\phi_c = 0.125$. The value of R is comparable to the measured R_g of the PE−PP chains, which is 126 Å.[1] It is evident that the simple equation proposed by Gompper and Schick provides a reasonable description of the data.

The effect of block copolymer concentration on the structure of phase-separated PE/PP/PE−PP blends with $\phi_{PE}/\phi_{PP} = 1.6$ is also depicted in Figure 18. The symbol M identifies systems that exhibited macrophase separation. The symbol O identifies systems that formed ordered microphases. The symbol Mi identifies systems that formed microemulsions, which, in the case of these PE/PP/PE−PP blends, coexisted with large-scale defects. The distinction between M and Mi phases in Figure 18 is clear, because q_{peak} is zero for M phases and finite

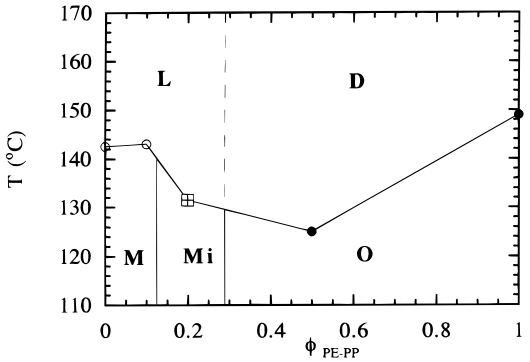

Figure 19. Experimentally determined phase diagram of the ternary PE/PP/PE−PP blends with $\phi_{PE}/\phi_{PP} = 1.6$, indicating macrophase-separated systems (M), microemulsions (Mi), ordered phases (O), liquidlike single-phase systems with no scattering peaks (L), and disordered single-phase systems with scattering peaks at finite scattering angles (D).

for Mi phases. In contrast, the distinction between Mi and O phases is more subtle. Consequently, our assignment of the location of the crossover between these phases is somewhat tentative. Both Mi and O phases are characterized by a single scattering peak. Moreover, q_{peak} is a smooth function of block copolymer concentration when ϕ_{PE-PP} exceeds ϕ_c. However, two vastly different asymptotic behaviors can be identified in Figure 18. In the limit of $\phi_{PE-PP} \rightarrow 1$, where we have identified ordered phases, the q_{peak} versus ϕ_{PE-PP} curve is nearly horizontal. In contrast, in the limit of $\phi_{PE-PP} \rightarrow f_c$, where we have identified microemulsions, the q_{peak} versus ϕ_{PE-PP} curve is nearly vertical. We have identified the crossover from microemulsions to ordered phases at $\phi_{PE-PP} = 0.289$ where the slope of the q_{peak} versus ϕ_{PE-PP} curve has a value that lies halfway between the two asymptotes. The slope of the Gompper−Schick curve at this point is equal to that of the line segment joining the two ends of the curve in Figure 18.

The phase diagram for PE/PP/PE−PP blends with $\phi_{PE}/\phi_{PP} \approx 1.6$ is shown in Figure 19. The data points represent experimentally determined phase transition points; open circles represent liquid−liquid phase transitions, filled circles represent order−disorder phase transitions, and the hatched square represents the microemulsion-to-disorder transition. These solid line segment joining these points divide the phase diagram into two regions: the single-phase region at high temperatures and the phase-separated region at low temperatures. Single-phase systems are of two types. The symbol L represents liquidlike blends in which the SANS profiles had their maximum in the forward direction. The symbol D represents disordered systems in which the SANS profiles had a scattering peak at finite scattering angles. The symbols M, Mi, and O are defined in the previous paragraph and in Figure 18. These assignments are based on scattering profiles obtained from the BH series. The experimental phase diagram (Figure 19) is in reasonable agreement with the theoretical phase diagram, given in Figure 15 of paper I,[1] especially when one considers the simplicity of the mean-field theory and the fact that the theoretical phase diagram was constructed without resorting to any measurements on multicomponent systems.

Concluding Remarks

We have conducted a systematic study of the thermodynamics of PE/PP/PE−PP blends using light and neutron scattering. PE and PP are incompatible polymers, and the PE−PP block copolymer can, in principle, serve as a polymeric surfactant. The addition of surfactants to incompatible oil/water mixtures results in the formation of microemulsions,[11−13] which have attracted considerable attention, due to their application in enhanced oil recovery. The ability of microemulsions to solubilize large amounts of oil, coupled with their low viscosity, make them ideal candidates for this application. The ordered phases, formed at higher surfactant concentrations, can also hold considerable amounts of oil, but high viscosity and solidlike properties of these systems makes them undesirable for oil recovery.

We have shown in this work that PE/PP/PE−PP blends exhibit phase behavior that is similar to that found in oil/water/surfactant mixtures. We have identified ordered, disordered, and microemulsion phases in these blends. Similar observations have been made on other polymer systems, particularly by Bates et al.[15] and by Jackson et al.[21] A better understanding of these phases may lead to a new class of polymer blends. For example, thermodynamically stable, periodic structures, may also be stable under certain flow conditions, thereby enabling a processing window that preserves the quiescent morphology. Ordered phases, which have not been commercially important in oil/water systems, may be useful in polymeric systems for structural applications that need solidlike properties. Thermoplastic elastomers, based on multicomponent systems, may be processed in the disordered state and used in the ordered state as soft solids. The presence of large amounts of homopolymers make these systems economically attractive.

The fundamental difference between the oil/water microemulsions and polymer microemulsions is the chainlike nature of the polymeric components. In small molecule systems, changing temperature and blend composition results mainly in intermolecular aggregation.[11−13,20,22] In polymer systems, we have observed both intermolecular and intramolecular effects. We found that the formation of disordered phases, ordered phases, and microemulsions is announced by pretransitional, intermolecular aggregation of the homopolymers. The ordering transition was also announced by intramolecular segregation of the PE and PP blocks of the copolymer as the ordering transition is approached. We were able to draw these conclusions due to our ability study individual chemical species in the multicomponent mixtures, by contrast matching.

The thermodynamics of microemulsion and order formation are dependent on a variety of factors such as the incompatibility of immiscible liquids, the amphiphilic strength of the surfactant, and properties of the internal interfaces such as interfacial energy and bending moduli.[11−13,22] In small molecule systems, these parameters are obtained by fitting experimental data to phenomenological theories. In principle, all the relevant quantities for periodic polymer structures can be estimated from the Flory−Huggins interaction parameter and chain statistics.[23,24] These systems may therefore provide stringent tests for thermodynamic theories.

From our work thus far on multicomponent blends we have obtained a reasonable understanding of single-phase systems. Most of the thermodynamic complexity that was observed for the PE/PP/PE−PP blends studied here was predicted by theories based on the random

phase approximation. Our previous studies[9,10,25] led us to the same conclusion. In contrast, our work on phase-separated systems[19,26,27] is far from complete. Recently, Schick and co-workers have used self-consistent field theory and simulations to study the phase behavior of mixtures of two homopolymers and a block copolymer.[28,29] These studies provide the motivation for a more complete characterization of the phase-separated systems. Many of the characteristics of phase-separated systems are dependent on the nature of the internal interfaces. Theoretical studies indicate that broad internal interfaces are necessary for microemulsion formation.[30] Such effects can be examined directly by studying thin films with the depth profiling techniques (for example, refs 31 and 32). We hope that these combined efforts will lead to a better understanding of the origin of order and disorder in multicomponent polymer blends.

Acknowledgment. Financial support from the National Science Foundation to Polytechnic University (DMR-9457950), the 3M Non-Tenured Faculty Award to N.P.B., and the Exxon Education Foundation is gratefully acknowledged. We thank the scientists at the National Institute of Standards and Technology[33] for their help with the SANS measurements. The 30 m SANS instrument is supported by the National Science Foundation under Agreement No. DMR-9423101. We thank Alessandro Faldi, Dave Lohse, Pratima Rangarajan, Glenn Reichart, and Charles Ruff for their help in characterizing the polyolefins, and the reviewers for their constructive criticism and valuable suggestions.

Note Added in Proof

While this paper was under review, three related papers appeared in print. Bates et al. have obtained electron micrographs of polymer microemulsions.[34] Kielhorn and Muthukumar have presented a theory that accounts for fluctuation corrections in mixtures of two homopolymers and a block copolymer.[35] A brief summary of our results on ordered PE/PP/PE−PP blends has also been published.[36]

References and Notes

(1) Jeon, H. S.; Lee, J. H.; Balsara, N. P. *Macromolecules* **1998**, *31*, 3328.
(2) de Gennes, P. G. *Scaling Concepts in Polymer Physics*; Cornell University Press: Ithaca, NY, 1979.
(3) Leibler, L. *Macromolecules* **1980**, *13*, 1602.
(4) Benoit, H.; Benmouna, M.; Wu, W. L. *Macromolecules* **1990**, *23*, 1511.
(5) Akcasu, A. Z.; Tombakoglu, M. *Macromolecules* **1990**, *23*, 607.
(6) Akcasu, A. Z.; Klein, R.; Hammouda, B. *Macromolecules* **1993**, *26*, 4136.
(7) Hammouda, B. *Adv. Polym. Sci.* **1993**, *106*, 87.
(8) de Gennes, P. G. *Faraday Discuss. Chem. Soc.* **1979**, *68*, 96.
(9) Balsara, N. P.; Jonnalagadda, S. V.; Lin, C. C.; Han, C. C.; Krishnamoorti, R. *J. Chem. Phys.* **1993**, *99*, 10011.
(10) Lin, C. C.; Jonnalagadda, S. V.; Balsara, N. P.; Han, C. C.; Krishnamoorti, R. *Macromolecules* **1996**, *29*, 661.
(11) de Gennes, P. G.; Taupin, C. *J. Phys. Chem.* **1982**, *86*, 2294.
(12) Gompper, G.; Schick, M. *Phys. Rev. B* **1990**, *41*, 9148.
(13) Teubner, M.; Strey, R. *J. Chem. Phys.* **1987**, *87*, 3195.
(14) Debye, P.; Bueche, A. M. *J. Appl. Phys.* **1949**, *20*, 518.
(15) Bates, F. S.; Maurer, W.; Lodge, T. P.; Schulz, M. F.; Matsen, M. W. *Phys. Rev. Lett.* **1995**, *75*, 4429.
(16) Broseta, D.; Fredrickson, G. H. *J. Chem. Phys.* **1990**, *93*, 2927.
(17) Leibler, L.; Benoit, H. *Polymer* **1981**, *22*, 195.
(18) Balsara, N. P.; Fetters, L. J.; Hadjichristidis, N.; Lohse, D. J.; Han, C. C.; Graessley, W. W.; Krishnamootri, R. *Macromolecules* **1992**, *25*, 6137.
(19) Lin, C. C.; Jeon, H. S.; Balsara, N. P.; Hammouda, B. *J. Chem. Phys.* **1995**, *103*, 1957.
(20) Trevino, S. F.; Joubran, R.; Parris, N.; Berk, N. F. *Langmuir* **1994**, *10*, 2547.
(21) Jackson, C. L.; Sung, L.; Han, C. C. *Polym. Eng. Sci.* **1997**, *37*, 1.
(22) Schubert, K. V.; Strey, R.; Klein, S. R.; Kaler, E. W. *J. Chem. Phys.* **1994**, *101*, 5345.
(23) Milner, S. T.; Witten, T. *J. Phys. (Fr.)* **1988**, *49*, 1951.
(24) Wang, Z. G.; Safran, S. A. *J. Phys. (Fr.)* **1990**, *51*, 185.
(25) Lin, C. C.; Jonnalagadda, S. V.; Kesani, P. K.; Dai, H. J.; Balsara, N. P. *Macromolecules* **1994**, *27*, 7769.
(26) Balsara, N. P.; Lin, C. C.; Hammouda, B. *Phys. Rev. Lett.* **1996**, *77*, 3847.
(27) Jeon, H. S.; Lee, J. H.; Balsara, N. P.; Majumdar, B.; Fetters, L. J.; Faldi, A. *Macromolecules* **1997**, *30*, 973.
(28) Holyst, R.; Schick, M. *J. Chem. Phys.* **1992**, *96*, 7728.
(29) Muller, M.; Schick, M. *J. Phys. Chem.* **1996**, *105*, 8885.
(30) Deem, M. W.; Chandler, D. *Phys. Rev. E.* **1994**, *49*, 4276.
(31) Dai, K. H.; Norton, L. J.; Kramer, E. J. *Macromolecules* **1994**, *27*, 1949.
(32) Shull, K. R.; Mayes, A. M.; Russell, T. P. *Macromolecules* **1993**, *26*, 3929.
(33) Certain equipment and instruments or materials are identified in this paper in order to adequately specify the experimental details. Such identification does not imply recommendation by the National Institute of Standards and Technology, nor does it imply the materials are necessarily the best available for the purpose.
(34) Bates, F. S.; Maurer, W. W.; Lipic, P. M.; Hillmyer, M. A.; Almdal, K.; Mortensen, K.; Fredrickson, G. H.; Lodge, T. P. *Phys. Rev. Lett.* **1997**, *79*, 849.
(35) Kielhorn, L.; Muthukumar, M. *J. Chem. Phys.* **1997**, *107*, 5588.
(36) Jeon, H. S.; Lee, J. H.; Balsara, N. P. *Phys. Rev. Lett.* **1997**, *79*, 3274.

MA9709720